

POST-TEST EXAMINATIONS OF A LOCA SAMPLE FROM AN IRRADIATED HIGH-BURNUP PWR M5 FUEL ROD

Y. YAN, J.M. HARP, K.D. LINTON

*Nuclear Energy and Fuel Cycle Division, Oak Ridge National Laboratory
One Bethel Valley Road, Oak Ridge, TN 37932 USA*

N. BROWN

*Department of Engineering Department, University of Tennessee
1412 Circle Drive, Knoxville, TN 37996 USA*

ABSTRACT

Loss-of-coolant-accident (LOCA) integral testing of a high-burnup PWR M5 fuel rod was conducted in the Irradiated Fuel Examination Laboratory through the complete LOCA sequence: heating the LOCA sample to 300°C and pressurizing the internal pressure to 8.27 MPa, heating at 5°C/s from 300 to 1200°C, holding in steam for 90s at 1200°C, cooling at 3°C/s to 800°C, followed by water quenching and rapid cooling to 100°C. After LOCA testing, examinations such as fuel fragmentation analysis, burst and ballooning characterization, axial strain measurement, and microstructural examination were performed. Metallographic examinations of an as-irradiated high-burnup sample adjacent to the LOCA test sample revealed a bonding layer between the fuel and cladding. The post-test LOCA examinations indicate the corrosion layer formed during normal operations in the commercial reactor might provide protection against steam oxidation at high temperatures for test times performed in this work. The microstructure of the as-irradiated fuel was compared with the microstructure of the post-LOCA test fuel. Post-test LOCA examination of unirradiated post-test Zr cladding samples was conducted and served as baseline data for in-cell testing with irradiated samples. The results obtained with irradiated high-burnup PWR M5 fuel rod were compared with the LOCA test data obtained with an irradiated BWR high-burnup Zircaloy-2 fuel rod at Argonne National Laboratory.

This manuscript has been authored by UT-Battelle, LLC, under contract DE-AC05-00OR22725 with the US Department of Energy (DOE). The US government retains and the publisher, by accepting the article for publication, acknowledges that the US government retains a nonexclusive, paid-up, irrevocable, worldwide license to publish or reproduce the published form of this manuscript, or allow others to do so, for US government purposes. DOE will provide public access to these results of federally sponsored research in accordance with the DOE Public Access Plan (<http://energy.gov/downloads/doe-public-access-plan>).

1. Introduction

The high-temperature steam oxidation behavior of zirconium alloy cladding under design-basis loss-of-coolant accidents (LOCAs) and over a broader set of conditions has been studied at several facilities around the world [1-7]. Oak Ridge National Laboratory (ORNL) is conducting

research on high-burnup pressurized water reactor (PWR) fuel with the Severe Accident Test Station (SATS), which is capable of testing nuclear fuel rods subjected to a range of accident scenarios [8-10]. The results from LOCA tests performed in the SATS will enable the industry and regulatory agencies to best address the LOCA phenomenon in standard light water reactor fuel designs irradiated to high burnup. The SATS consists of two modules focused on assessing the performance of materials in design-basis accident (DBA) and beyond-design-basis-accident (BDBA) conditions, respectively. DBA evaluation is conducted using the LOCA Test System originally developed at Argonne National Laboratory (Argonne). It has played an essential role in formulating the most recent set of regulatory test criteria from the U.S. Nuclear Regulatory Commission with respect to DBA LOCAs. The SATS replicates and optimizes the already demonstrated Integral LOCA Test System to simulate BDBA conditions at much higher temperatures than the Integral LOCA Test System can. The post-test examination of a LOCA sample from irradiated high-burnup M5 fuel rod is reported in this work.

2. Materials and Experimental

A high-burnup PWR North Anna (NA) M5 fuel segment at ≈ 70 GWd/MTU was used for LOCA integral testing. Approximately 13 mm of fuel was removed from both ends of the specimen. Following end-cap welding, the fuel specimen was attached by Swagelok fittings and then assembled to the test train [8]. Two Type-S thermocouples were strapped to the outer surface of the cladding approximately 50 mm above the sample centerline. One of them was used to control the sample temperature. A comparison between the welded and strapped thermocouples indicated less than a 10°C difference in readings. The in-cell LOCA integral test was conducted in steam in a full sequence, which included heating the fuel segment in flowing steam to 300°C , internally pressurizing it to 8.27 MPa at 300°C , increasing the temperature to $1,200^\circ\text{C}$ at 5°C/s , holding in steam for 90 s at $1,200^\circ\text{C}$, cooling at 3°C/s to 700°C , and furnace cooling from 700°C to $\approx 100^\circ\text{C}$. After LOCA testing, post-test examinations were performed. Table 1 summarizes the test parameters of the LOCA tests in this work.

3. Results

3.1 Fuel morphology and fragmentation

Before LOCA testing, pre-test characterization was performed on two specimens sectioned from both ends of the LOCA specimen to measure the corrosion layer thickness and fuel-cladding-bond layer thickness. Figure 1 shows high-magnification micrographs of the corrosion layer on the outer surface and the fuel-cladding-bond layer on the inner surface. Micrographs were taken at eight azimuthal locations (every 45 degrees) of the cross section of the MET mounts and were analyzed for layer thickness. The thickness of the outer surface corrosion layer was uniform and well defined (see Figure 1a). Based on the images at eight circumferential locations, the corrosion layer thickness was determined to be $7 \pm 2 \mu\text{m}$. Because of the highly nonuniform bond-fuel interface (see Figure 1b), the reported bond thickness of $13 \pm 3 \mu\text{m}$ is that of an equivalent oxide bond with a smooth fuel interface.

Figure 2a shows the post-test fuel rod and fuel fragments from NA#1. The total amount of fuel collected from NA#1 was 28.5 g. Sieve analysis was performed. The fragment size distribution of the fuel collected after LOCA fragmentation and shake testing of the NA#1 sample was quantified, and the result is shown in Figure 2b. The fuel morphology for the post-test NA#1 at locations 50 mm below the burst midplane is shown in Figure 3b; it can be compared with the fuel morphology of the as-irradiated rod (Figure 3a). The cladding strain at 32.5 mm below the burst is 2.9%. Most of the fuel appears to have pulled away from the cladding at 32.5 mm below the burst.

Parameter	NA#1	Zr4-23	Zr4-22
Alloy	M5	Zircaloy-4	Zircaloy-4
Internal Pressure at 300°C, MPa	8.27	4.14	8.27
Temperature Ramp from 300°C, °C/s	5	5	5
Peak Internal Pg, MPa	8.37	4.37	8.46
Temperature at Burst, °C	791	866	790
Hold Temperature, °C	1200	1200	1200
Hold Time, seconds	90	135	90
Cool-Down Rate to 800°C, °C/s	3	3	3
Quench Initiation Temperature, °C	700	700	700
Burst Shape	Oval	Dog Bone	Dog Bone
Burst Length, mm	16	7	9
Max. Burst Width, mm	3.0	1.8	2.5
Max. Strain ($\Delta C/C_m$) _{max} , %	38	27	47
Wall Thickness for ECR Calculation, mm	0.57	0.57	0.57

Table 1 Parameters of LOCA tests with Unirradiated Cladding and High-burnup Fuel Rod Segment

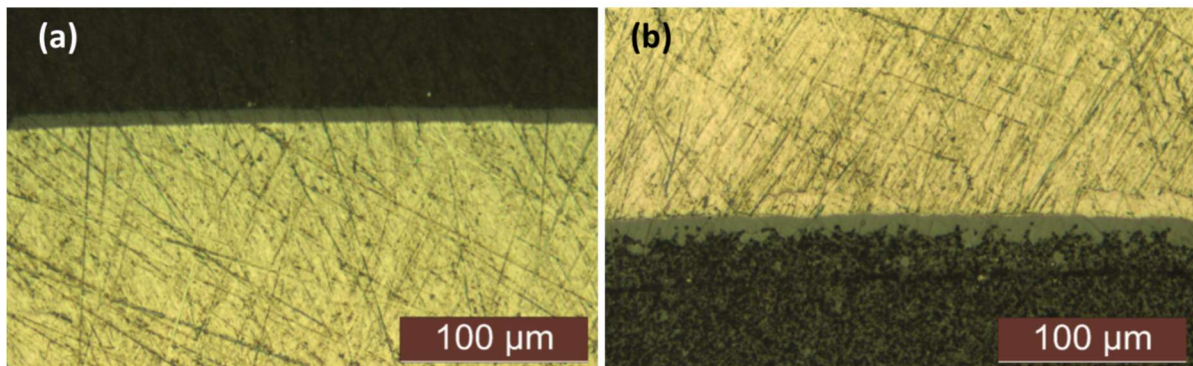


Figure 1. (a) Corrosion layer (dark gray) on pre-test M5 cladding outer surface. Based on images at eight circumferential locations, the corrosion layer thickness was determined to be $7 \pm 2 \mu\text{m}$. (b) Fuel-cladding-bond oxide layer (dark gray) on M5 cladding inner surface; the bond layer thickness was determined to be $13 \pm 3 \mu\text{m}$.

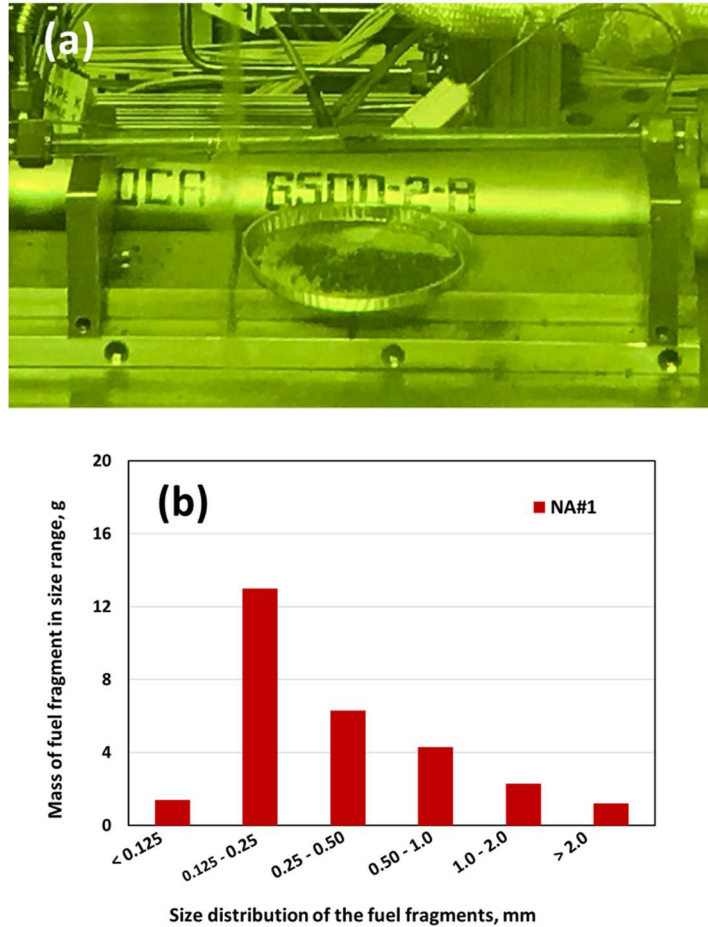


Figure 2. (a) Post-test NA#1 test specimen with fuel particles that fell out of the burst opening. (b) Size distribution of fuel fragments collected after LOCA test NA#1. The total fuel collected in the pan is 28.5 g.

3.2 Ballooning and burst of post-test LOCA samples

The specimen NA#1 was tested in a full LOCA sequence similar to the testing conditions for ICL#4, which was tested at Argonne. Although the cladding geometry and cladding material are different between these tests, their burst temperatures were remarkably close. A profile of diametral strain for NA#1 is shown in Figure 4. It is compared with results from a companion LOCA test with unirradiated Zircaloy-4 sample Zr4 #22 in Figure 4a (tested under the same conditions as NA#1) and with results from ANL LOCA test ICL#1 with a high-burnup BWR Limerick fuel rod (Figure 4b).

The primary differences observed between the high-burnup M5 cladding and the unirradiated Zircaloy-4 cladding were in pre-burst bending (which was less for high-burnup specimen), maximum opening (large for high-burnup specimen), and maximum strain (less for high-burnup specimen). However, the maximum strain for the ORNL NA#1 and the Argonne ICL#4 specimens were remarkably close, although the axial extent of the balloon region was different between the two tests (less for the Argonne data). In Figure 5, the post-test LOCA samples NA#1 and Zr4#22 are shown. The opening of unirradiated sample Zr4#22 has a fish-mouth shape (Figure 5b), and the irradiated sample NA#1 has an oval opening (Figure 5a). These results are consistent with Argonne data (see Figure 5c and 5d).

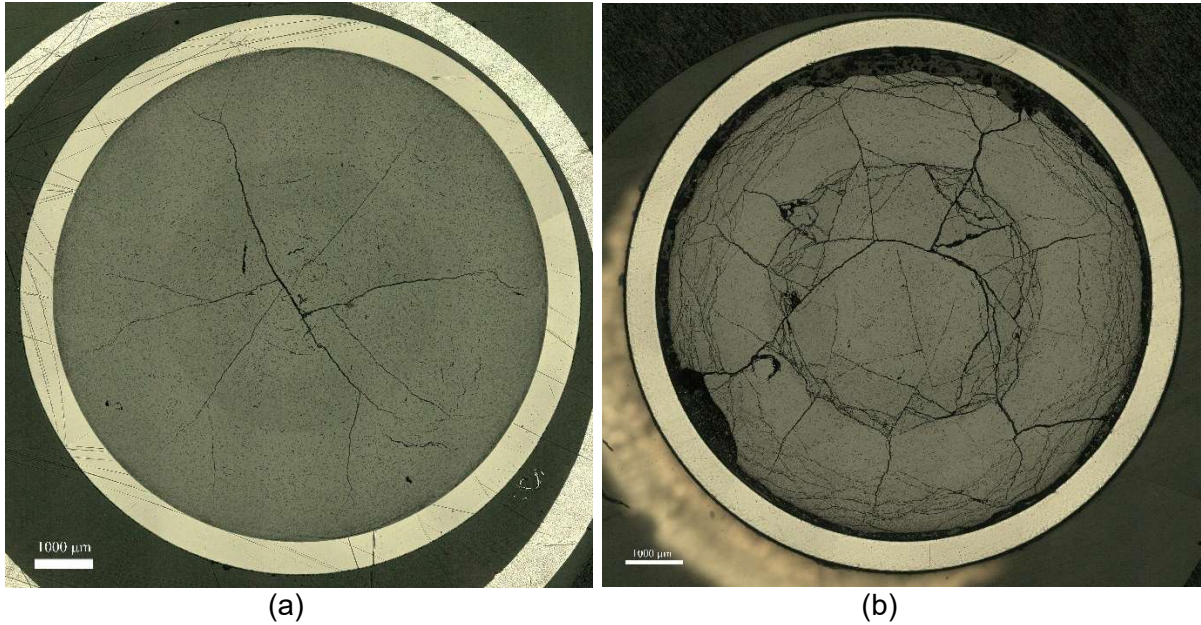


Figure 3. Fuel morphology for the North Anna M5 high-burnup LOCA sample NA#1: (a) as-irradiated, pre-test condition; (b) post-test condition at 32.5 mm below burst midplane.

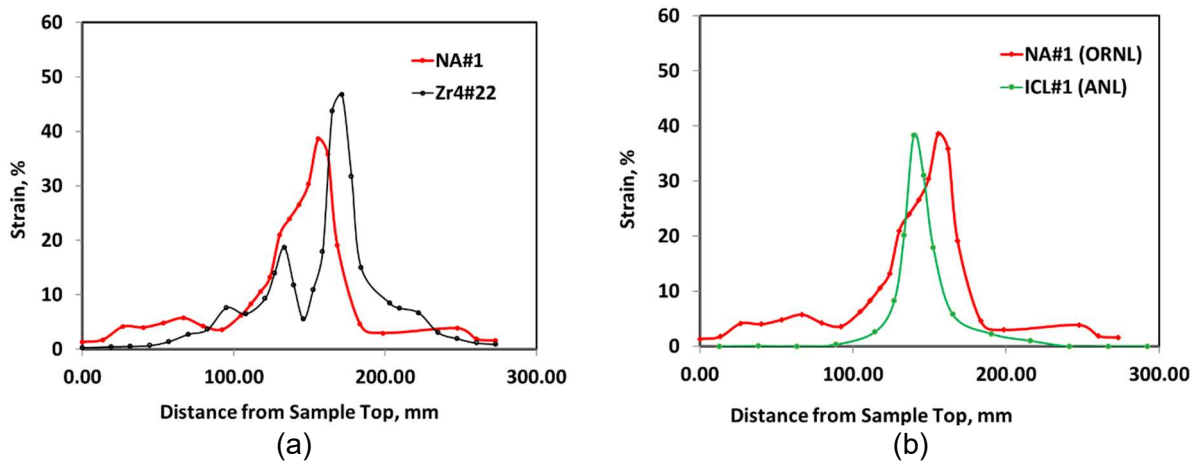


Figure 4. Outer-diameter strain for ORNL LOCA integral test NA#1 (red line) compared with a companion LOCA test, Zr4 #22, with unirradiated Zircaloy-4 (a) and with Argonne LOCA test ICL#1 [4] with a high-burnup BWR Limerick fuel rod (b). The Zr4#22 was tested under the same conditions as the NA#1.

Histories for pressure and time during the ramp for NA#1 are shown in Figure 6. The pressure increased from 8.27 MPa to a maximum of 8.37 MPa during heating and decreased to 8.24 MPa just before burst. Figure 6a shows a pressure history for NA#1A compared with a companion test Zr4#22 with unirradiated Zircaloy-4 cladding. The pressure decreased very fast for Zr4#22 but much more slowly for the high-burnup sample NA#1. Figure 6b shows a comparison of the pressures between the ORNL NA#1 and Argonne ICL#1 specimens. The pressure drop of the NA#1 sample was slower than for the ICL#1. However, the results indicate that high-burnup NA#1 fuel still has sufficient permeability to gas flow to sustain the growth of the balloon through the burst phase, as confirmed by the maximum strains shown in Figure 4b.

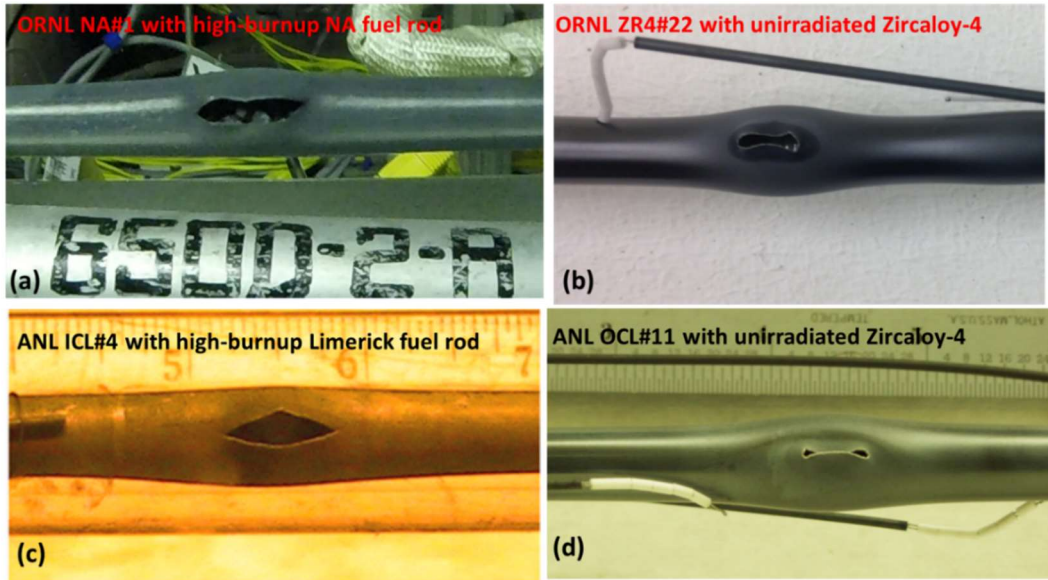


Figure 5. Comparison of burst openings for ORNL and Argonne LOCA specimens [4].

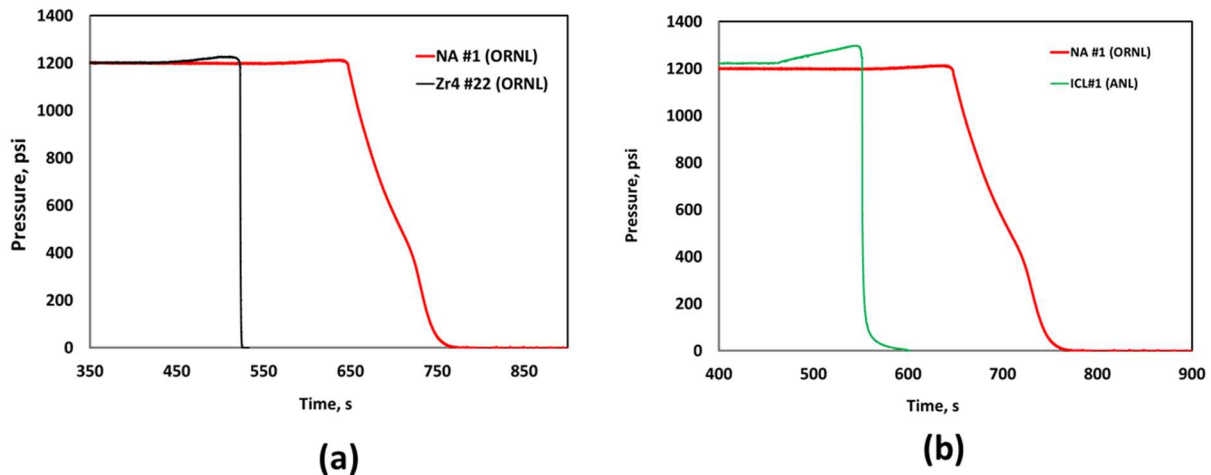


Figure 6. Pressure and temperature histories for the ORNL LOCA integral test NA#1 (red line) compared with pressure history for (a) companion test Zr4 #22 (black line) with unirradiated Zircaloy-4, and (b) Argonne LOCA test ICL#1 [4] with high-burnup BWR Limerick fuel rod.

3.3 Oxidation and hydrogen pickup due to secondary hydriding

For the NA#1 sample, metallographic characterization was performed at the burst midplane (Figure 7) and 50 mm above the midplane (Figure 8) to determine the degree of steam oxidation (two-sided vs. one-sided and outer diameter vs. inner diameter oxide layer thickness within the balloon region). Two-sided oxidation was observed at the midplane. The outer oxide layer thickness (averaged from eight locations) was $30.0 \pm 6.2 \mu\text{m}$ and the inner oxide layer thickness was $29.8 \pm 4.6 \mu\text{m}$. However, the inner surface oxide layer was much thinner than the outer surface oxide layer at the axial location 50 mm above the burst midplane because the fuel blocked the steam access to the inner surface. The measured outer oxide layer thickness was $30.6 \pm 5.7 \mu\text{m}$ and the inner oxide layer thickness was $\leq 5 \mu\text{m}$ at the 50 mm axial location.

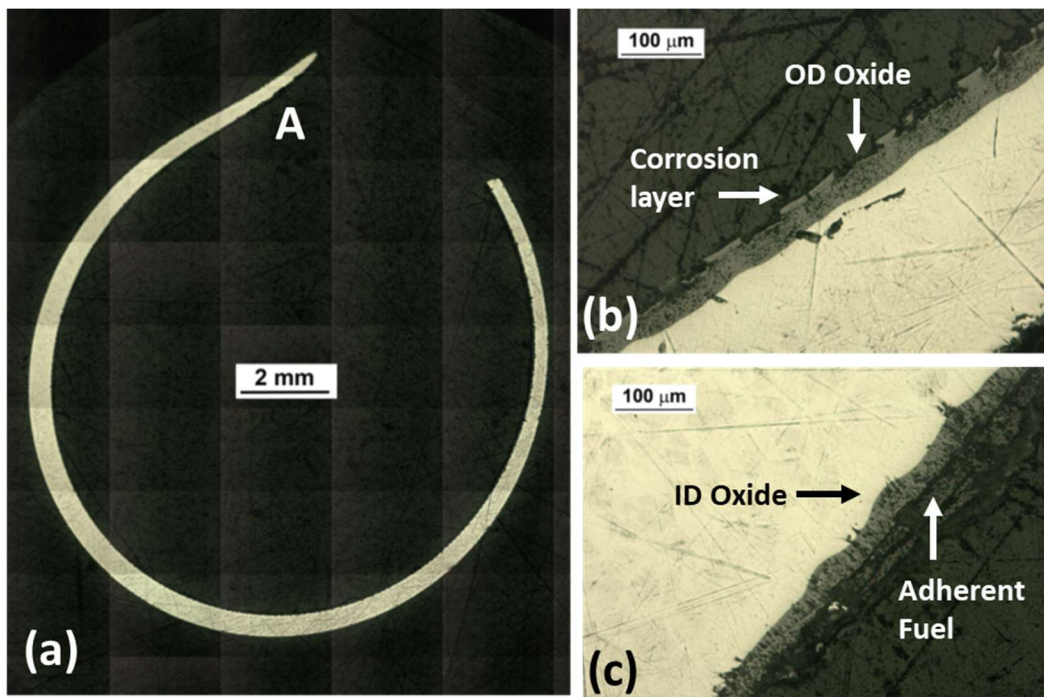


Figure 7. Cladding cross section at burst midplane for NA#1 sample at low magnification (left) and at high magnification (right) showing the outer-diameter and inner-diameter oxide layers at location A of Figure 7a. Note the wavy interfaces.

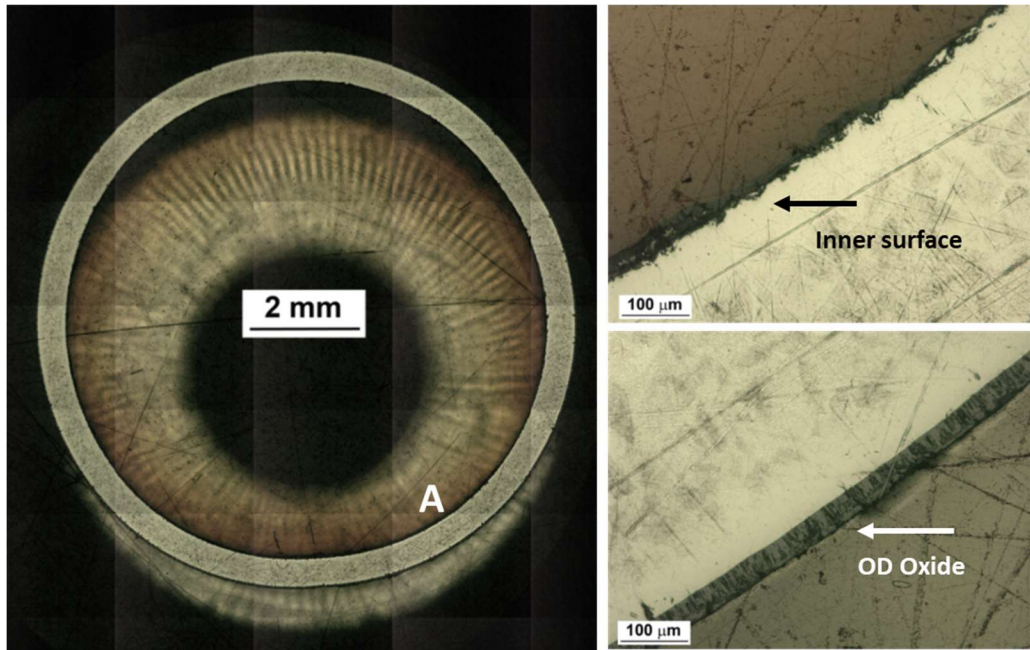


Figure 8. Cladding cross section 50 mm above the burst midplane for NA#1 sample at low magnification (left) and high magnification (right) showing the outer-diameter and inner-diameter oxide layers at location A. Note the lack of wavy interfaces on OD surface.

The cladding strain at the midplane was 38.6% and the cladding strain at 50 mm above the midplane was \approx 6.3%. Most of the fuel appeared to have pulled away and have been lost from the midplane. The high cladding strain broke the outer-diameter corrosion later, causing waved oxide layers to form during high-temperature steam oxidation (see Figure 7b). This finding indicates that the corrosion layer formed during normal operation in the reactor might provide protection against high-temperature steam oxidation for the test times used in this work.

As a result of steam leakage through the burst opening, oxidation within the balloon region was two-sided, as discussed earlier. The oxidation resulted in hydrogen release to the near-stagnant steam within the test sample. Unlike the case for the outer surface exposed to flowing steam, a large fraction of the released hydrogen was trapped inside the sample and available for pickup by the inner-metal surface in and near the balloon region. Figure 9 shows LECO-measured hydrogen content vs. strain distribution for a control test, Zr4#23, an unirradiated Zircaloy-4 sample oxidized for 90 s at 1200°C. The hydrogen distributes symmetrically about the burst midplane. The maximum content is 2769 wppm at \approx 27 mm below the midplane, where the cladding strain is 9.6%. The magnitude of the hydrogen pickup was quite large for such a short hold time at 1200°C, indicating that significant hydrogen pickup occurred early in the LOCA transient. Enough hydrogen was released to the cladding interior as a result of inner-surface oxidation during the ramp to result in high hydrogen pickup. We expect to measure the hydrogen and oxygen pickups for the high-burnup LOCA sample NA#1 in the near future.

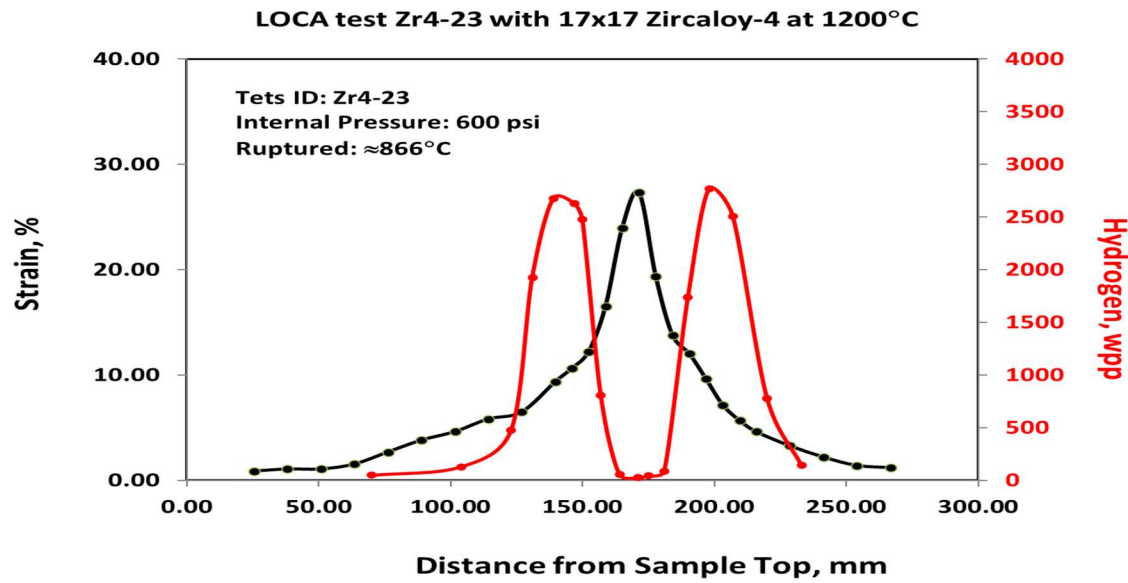


Figure 9. LECO hydrogen content and ballooning strain profile for unirradiated control ORNL-Zr4#23 sample ramped in steam from 300°C.

4. Conclusion

This paper summarized the initial post-test examinations of LOCA samples of an irradiated high-burnup M5 fuel rod. The permeability of high-burnup NA M5 fuel, as well as the plastic expansion of the cladding away from the fuel, was sufficient to sustain ballooning out to a maximum circumferential strain of 39% and to induce burst at \approx 790°C and \approx 8.4 MPa internal pressure. Those values are consistent with those obtained from companion out-of-cell tests using unirradiated Zircaloy-4 specimens and with LOCA data from Argonne. Fuel fragmentation analysis was performed. The results from integral LOCA tests provided valuable data for code and modeling validation, which enhances the ability to predict the behavior of fuel systems during

accident scenarios. Validation of nuclear fuel performance codes will provide results that can either act as a screening tool for future experiments or be coupled with experimental data to validate the behavior of a fuel system during safety testing.

5. References

1. J. V. Cathcart, R. E. Pawel, R. A. McKee, R. E. Druschel, G. J. Yurek, J. J. Cambell, and S. H. Jury, "Zirconium Metal-Water Oxidation Kinetics: IV. Reaction Rate Studies," ORNL/NUREG-17 (Aug. 1977).
2. Y. Yan, R. V. Strain, T. S. Bray, and M. C. Billone, "High Temperature Oxidation of Irradiated Limerick BWR Cladding," NUREG/CP-0176 (May 2002), 353-372.
3. F. Nagase, T. Otomo, and H. Uetsuka, "Oxidation Kinetics of Low-Sn Zircaloy at the Temperature Range from 773 to 1571K," Nucl. Sci. & Tech. 40 (2003) 213-219.
4. M. Billone, Y. Yan, T. Burtseva, and R. Daum, "Cladding Embrittlement during Postulated Loss-of-Coolant Accidents," NUREG/CR-6967, ANL-07/04 (July 2008).
5. J.-P. Mardon, D. Charquet, and J. Senevat, "Influence of Composition and Fabrication Process on Out-of-Pile and In-Pile Properties of M5 Alloy," Zirconium in the Nuclear Industry: 12th International Symposium, ASTM STP 1354, G. P. Sabol and G. D. Moan, Eds., American Society for Testing and Materials, West Conshohocken, PA, (2000), 505-524.
6. R. J. Comstock, G. Schoenberger, and G. P. Sabol, "Influence of Processing Variables and Alloy Chemistry on the Corrosion Behavior of ZIRLO Nuclear Fuel Cladding," Zirconium in the Nuclear Industry: 11th International Symposium, ASTM STP 1295, E. R. Bradley and G. P. Sabol, Eds., American Society for Testing and Materials (1996), 710-725.
7. Y. Yan, T. Burtseva, and M. Billone, "High-temperature steam-oxidation behavior of Zr-1Nb cladding alloy E110" J. Nuclear Materials, 393 (2009), 433–448.
8. Yong Yan, Zachary Burns, Kory Linton, and Kurt A. Terrani, "Results from In-cell Integral LOCA Testing at ORNL," WRFPM 2017 (September 2017), Jeju Island, South Korea.
9. Yong Yan, Zach Burns, Tyler Smith, Kory Linton, Ken Yueh, and Kurt Terrani, "LOCA Fragmentation Test with High Burnup HBR Fuel Rod" ORNL/TM-2019/1239 (October 2019).
10. Nathan Capps, Yong Yan, Alicia Raftery, Zachary Burns, Tyler Smith ,Kurt Terrani, Ken Yueh, Michelle Bales, and Kory Linton, "Integral LOCA fragmentation test on high-burnup fuel" Nuclear Engineering and Design, 369 (2020), 110811.